

# A physically-based model for the electrical conductivity of water-saturated porous media

Luong Duy Thanh<sup>1\*</sup>, Damien Jougnot<sup>2</sup>, Phan Van Do<sup>1</sup>, Nguyen Van Nghia A<sup>1</sup>

(1) Thuyloi University, 175 Tay Son, Dong Da, Ha Noi, Vietnam

(2) Sorbonne Université, CNRS, EPHE, UMR 7619 Metis, F-75005, Paris, France

(\*)Corresponding author: thanh\_lud@tlu.edu.vn

arXiv:1908.10601v1 [physics.geo-ph] 28 Aug 2019

This paper has been published in Geophysical Journal International, please cite as:  
Luong Duy Thanh, Damien Jougnot, Phan Van Do, Nguyen Van Nghia A, A physically based model for the electrical conductivity of water-saturated porous media, Geophysical Journal International, Volume 219, Issue 2, November 2019, Pages 866–876, <https://doi.org/10.1093/gji/ggz328>

## Abstract

Electrical conductivity is one of the most commonly used geophysical method for reservoir and environmental studies. Its main interest lies in its sensitivity to key properties of storage and transport in porous media. Its quantitative use therefore depends on the efficiency of the petrophysical relationship to link them. In this work, we develop a new physically based model for estimating electrical conductivity of saturated porous media. The model is derived assuming that the porous media is represented by a bundle of tortuous capillary tubes with a fractal pore-size distribution. The model is expressed in terms of the porosity, electrical conductivity of the pore liquid and the microstructural parameters of porous media. It takes into account the interface properties between minerals and pore water by introducing a surface conductivity. Expressions for the formation factor and hydraulic tortuosity are also obtained from the model derivation. The model is then successfully compared with published data and performs better than previous models. The proposed approach also permits to relate the electrical conductivity to other transport properties such as the hydraulic conductivity.

**Keywords:** Electrical conductivity; Formation factor; Fractal; Porous media

# 1 Introduction

Measuring electrical conductivity of rocks is of critical importance for oil and mineral exploration [e.g., Glover, 2009, Speight, 2011] and environmental studies [e.g., Hubbard & Rubin, 2005, Revil et al., 2012, Binley et al., 2015]. Geoelectrical measurements are a useful, nondestructive tool for characterizing porous rocks and soils [e.g., Binley & Kemna, 2005, Glover, 2015]. Conduction of electricity through porous media occurs by two mechanisms: (1) the primary mode of conduction is by movement of ions through the bulk saturating electrolyte and (2) it can also take place in the vicinity of solid surface of pores and cracks [e.g., Bussian, 1983, Revil & Glover, 1997, Revil et al., 1999] and that is termed the surface conductance. Surface conductivity includes conduction associated with electrical double layer (EDL): the Stern and diffuse layers and with proton transfer at the interface between the mineral and the pore water [e.g., Revil & Glover, 1997, 1998, Revil et al., 1999]. To characterize the relative contribution of the surface conductivity, the dimensionless quantity termed the Dukhin number ( $Du$ ) has been introduced. The Dukhin number is the ratio of the surface conductivity  $\sigma_s$  to the pore water conductivity  $\sigma_w$  as  $Du = \sigma_s/\sigma_w$  [Dukhin & Shilov, 1974]. The conductivity of a fully saturated porous medium is related to microstructural properties such as porosity, pore geometry, surface morphology of the mineral grains, pore fluid, temperature [Friedman, 2005, Glover, 2009]. For brine-saturated porous materials, Archie [1942] proposed an empirical relationship that links the formation factor  $F$  to the porosity  $\phi$  based on experimental measurements of electrical conductivity of saturated porous media  $\sigma$  and the electrical conductivity of the pore water  $\sigma_w$  as follows:

$$F = \lim_{\sigma_s \rightarrow 0} \left( \frac{\sigma_w}{\sigma} \right) = \phi^{-m}, \quad (1)$$

where  $m$  is called the cementation exponent that is supposed to be constant for a certain type of rock. The cementation exponent  $m$  is normally between 1.3 and 2.5 for unconsolidated sands, porous sediments and higher than 2.5 for carbonate rocks where the pore space is not well connected [e.g., Friedman, 2005, Glover, 2009, Glover et al., 1997]. Archie's law is playing an important role in the exploration of oil reservoir [e.g., Glover, 2009, Carpenter et al., 2009]. The electrical conductivity  $\sigma$  of saturated porous media for negligible surface conductivity can be obtained from Eq. (1) as

$$\sigma = \sigma_w \phi^m. \quad (2)$$

Beside the Archie model, many models are available in literature [e.g., Friedman, 2005, Laloy et al., 2011, Cai et al., 2017] to link the electrical conductivity of saturated porous media  $\sigma$  and the electrical conductivity of the pore fluid  $\sigma_w$ . For example, many relationships between  $\sigma$  and  $\sigma_w$  have been obtained from the effective medium theories [e.g., Bussian, 1983, Sen et al., 1981b, McLachlan et al., 1987, Ellis et al., 2010], the percolation theory [Hunt, 2004, Ghanbarian et al., 2014], the cylindrical tube model [Herrick & Kennedy, 1994], among other approaches. Existing electrical models with surface conductivity based on different approaches such as the two-resistors in parallel approach [e.g., Waxman & Smits, 1968, Brovelli et al., 2005], the effective medium [e.g., Hanai, 1961, Bussian, 1983], the volume averaging theorem [e.g., Pride, 1994, Linde et al., 2006] have also been presented in literature. Recently, fractal models have been proven to be

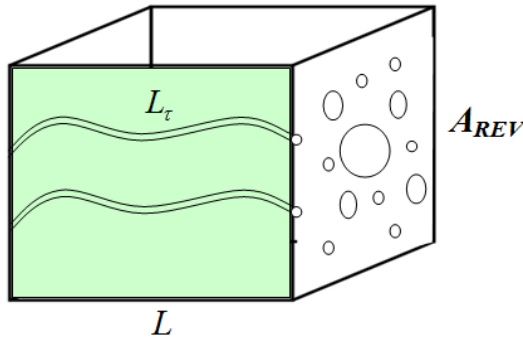


Figure 1: A porous rock model composed of a large number of parallel capillary tubes with radius following a fractal distribution.

an alternative and useful means for studying the transport phenomenon and analyzing the macroscopic transport properties of porous media [e.g., Mandelbrot, 1982, Thompson et al., 1987, Feder & Aharony, 1989, Thompson, 1991, Sahimi, 1993, Ghanbarian-Alavijeh et al., 2011, Xu, 2015, Thanh et al., 2018, Guarracino & Jougnot, 2018]. Fractal theory in porous media has been applied to derive theoretical electrical conductivity models [e.g., Katz & Thompson, 1985, Pape et al., 1987, Roy & Tarafdar, 1997, Coleman & Vassilicos, 2008a,b, Wei et al., 2015]. However, to the best of our knowledge, the surface electrical conductivity is not yet taken into account in the fractal electrical conductivity models that are already published. Therefore, one may underestimate electrical conductivities of saturated porous media and fail to reproduce experimental data when the electrical conductivity of the pore fluid is low.

In this work, we propose a fractal model for the electrical conductivity of saturated porous media based on the fractal theory of porous media and on the capillary bundle model. The proposed model is expressed in terms of microstructural parameters such as the minimum and maximum pore/capillary radii, the pore fractal dimension, the tortuosity fractal dimension and the porosity of porous media. The model prediction is then compared with experimental data in the literature. A good agreement is found between the prediction by the proposed fractal model and experimental data. Factors influencing the electrical conductivity in porous media are also analyzed.

## 2 Fractal theory for porous media

Fractal theory for porous media has been already presented by many works [e.g., Yu & Cheng, 2002a, Liang et al., 2014, 2015] in which a porous medium is assumed to be made up of an array of tortuous capillaries with different sizes (see Fig. 1). The pore size distribution in porous media has been proven to follow the fractal scaling law

$$N(\geq r) = \left(\frac{r_{max}}{r}\right)^{D_f}, \quad (3)$$

where  $N$  is the number of capillaries (whose radius  $\geq r$ ) in a fractal porous media,  $r_{max}$  is the maximum radius of capillary,  $D_f$  is the fractal dimension for pore space,  $0 < D_f < 2$  in two-dimensional space and  $0 < D_f < 3$  in three dimensional space [Yu & Cheng, 2002a,

Liang et al., 2014, 2015]. Eq. (3) implies the property of self-similarity of porous media, which means that the value of  $D_f$  from Eq. (3) remains constant across a range of length scales. It should be noted that porous media are not exactly self-similar. Porous media are shown to be statistically self-similar because they exhibit the self-similarity in some average sense and over a certain range of length scales [e.g., Yu et al., 2001, Yu & Cheng, 2002a]. As there are numerous capillaries in porous media, Eq. (3) can be considered as a continuous function of the radius.

Differentiating Eq. (3) with respect to  $r$  yields

$$-dN = D_f r_{max}^{D_f} r^{-D_f-1} dr, \quad (4)$$

where  $-dN$  represents the number of pores from the radius  $r$  to the radius  $r + dr$ . The minus (-) in Eq. (4) implied that the number of pores decreases with the increase of pore size. Therefore, the total number of capillaries from the minimum radius  $r_{min}$  to the maximum radius  $r_{max}$  can be obtained by

$$N_{total}(\geq r_{min}) = \left(\frac{r_{max}}{r_{min}}\right)^{D_f}. \quad (5)$$

From Eq. (4) and Eq. (5), we obtain

$$-\frac{dN}{N_{total}} = D_f r_{min}^{D_f} r^{-D_f-1} dr = f(r) dr, \quad (6)$$

where  $f(r) = D_f r_{min}^{D_f} r^{-D_f-1}$  is the probability density function of the pore size distribution. This function must satisfy the following condition

$$\int_{r_{min}}^{r_{max}} f(r) dr = 1 - \left(\frac{r_{min}}{r_{max}}\right)^{D_f} = 1 \quad (7)$$

or

$$\left(\frac{r_{min}}{r_{max}}\right)^{D_f} \approx 0. \quad (8)$$

As stated in Yu & Cheng [2002a], Liang et al. [2014] and Liang et al. [2015], for example, Eq. (8) holds approximately when  $r_{min}/r_{max} \approx 10^{-2}$  or  $< 10^{-2}$  in porous media. Generally, the above condition holds in porous media. Therefore, the fractal theory can be used to investigate properties of porous media [e.g., Katz & Thompson, 1985, Yu et al., 2001, Yu & Cheng, 2002b]. The fractal dimension for pore space ( $D_f$ ) is expressed as [e.g., Yu et al., 2001, Yu & Cheng, 2002a]

$$D_f = 2 - \frac{\ln \phi}{\ln \alpha}, \quad (9)$$

where  $\phi$  is the porosity of porous media and  $\alpha$  is the ratio of the minimum pore radius to the maximum pore radius ( $\alpha = r_{min}/r_{max}$ ).

### 3 Theoretical development of a new electrical model

#### 3.1 Pore scale

If the capillary radius is  $r$  and its length is  $L_\tau$  and if it is filled with a fluid of conductivity  $\sigma_w$ , then the resistance ( $R_c$ ) of the capillary should be [Street, 1961]

$$\frac{1}{R_c} = \frac{\pi r^2 \sigma_w}{L_\tau}, \quad (10)$$

However, if there is a contribution from surface conductance (specific surface conductance  $\Sigma_s$ ), then the resistance ( $R_s$ ) due to the surface conductance (i.e. the EDL) would be

$$\frac{1}{R_s} = \frac{2\pi r \Sigma_s}{L_\tau}, \quad (11)$$

It should be noted that  $\Sigma_s$  is related to the cationic exchange capacity of the porous medium [Revil et al., 1998, Woodruff & Revil, 2011].

The total resistance of the capillary (the two conductors in parallel) is given by [see Pfannkuch, 1972, for more details]

$$\frac{1}{R(r)} = \frac{1}{R_c} + \frac{1}{R_s} = \frac{\pi r^2 \sigma_w}{L_\tau(r)} + \frac{2\pi r \Sigma_s}{L_\tau(r)}. \quad (12)$$

One of the assumptions behind Eq. (12) is the percolation of the surface-conductive layer. This assumption is made in widely used models from the literature [e.g., Waxman & Smits, 1968, Pride, 1994, Gueguen & Palciauskas, 1994, Linde et al., 2006, Revil et al., 1998].

When this is not the case, one has to use different models such as self-similar up-scaling techniques [e.g., Sen et al., 1981a] or the percolation theory [e.g., Ghanbarian et al., 2014].

The relationship between the radius and length of the capillary should conform to the following fractal scaling relationship [e.g., Yu & Cheng, 2002b, Wu & Yu, 2007]

$$L_\tau(r) = r^{1-D_\tau} L_o^{D_\tau}, \quad (13)$$

where  $D_\tau$  is the fractal dimension for the geometrical tortuosity of the capillaries with  $1 < D_\tau < 2$  in two dimensions,  $L_o$  is the length of the porous media and  $L_\tau$  is the tortuous length.

From Eq. (13), the geometrical tortuosity of a capillary having a radius  $r$  is obtained as

$$\tau(r) = \frac{L_\tau(r)}{L_o} = \left(\frac{L_o}{r}\right)^{D_\tau-1}. \quad (14)$$

Eq. (14) indicated that smaller diameter capillaries are more tortuous than larger ones. That is consistent with the physical situation for an artery and micro-blood vessel. The artery is much larger in diameter but much less tortuous than the blood vessel [Bo-Ming, 2005, Doyen, 1988]. It should be noted that at the microscale, tortuosities can be either geometrical or electrical, or hydraulic. They are dependent of the capillary size as shown by Eq. (14). At the microscopic scale, we define the geometrical tortuosity ( $\tau_g$ ) as the

ratio between the effective shortest possible length between inflow and outflow points that avoid solid grains (this is realized as a zigzag path passing grains with close tangents) and the straight line length in the direction of flow in porous media [Clennell, 1997]. Hydraulic tortuosity ( $\tau_h$ ) is defined as the ratio of the effective fluid path length between solid grains (this is realized as a smoothed route through porous media) and the straight line length in the direction of flow [Clennell, 1997]. Electrical tortuosity ( $\tau_e$ ) is defined as the ratio of the effective path length for electrical flow and the straight line length of porous media [Clennell, 1997]. It is seen that  $\tau_g < \tau_e < \tau_h$  [Ghanbarian et al., 2013]. Note that, at the macroscale scale (i.e., REV scale described in the next section), these tortuosities become effective tortuosities (denoted "eff"): geometrical ( $\tau_g^{eff}$ ), electrical ( $\tau_e^{eff}$ ), and hydraulic ( $\tau_h^{eff}$ ). That is, they result from the analytical up-scaling of the tortuosities of many capillaries sizes described in the next section.

### 3.2 REV scale

In order to derive the electrical conductivity at macroscale, we consider a representative elementary volume (REV) as a cube with the length of  $L_o$  and the cross-section area of the REV perpendicular to the flow direction of  $A_{REV}$ . The porous medium of the REV is conceptualized as an equivalent bundle of capillary tubes with a fractal pore size distribution and the pore structure with radii varying from a minimum pore radius  $r_{min}$  to a maximum pore radius  $r_{max}$  as described in the previous section.

The resistance of the water-saturated rock in the REV can be obtained as [Jackson, 2008, 2010, Wang et al., 2014]

$$\begin{aligned} \frac{1}{R_o} &= \int_{r_{min}}^{r_{max}} \frac{1}{R(r)} (-dN) \\ &= \int_{r_{min}}^{r_{max}} \left( \frac{\pi r^2 \sigma_w}{r^{1-D_\tau} L_o^{D_\tau}} + \frac{2\pi r \Sigma_s}{r^{1-D_\tau} L_o^{D_\tau}} \right) D_f r_{max}^{D_f} r^{-D_f-1} dr \\ &= \frac{\pi \sigma_w D_f r_{max}^{D_\tau+1}}{L_o^{D_\tau} (D_\tau - D_f + 1)} (1 - \alpha^{D_\tau - D_f + 1}) + \frac{2\pi \Sigma_s D_f r_{max}^{D_\tau}}{L_o^{D_\tau} (D_\tau - D_f)} (1 - \alpha^{D_\tau - D_f}) \end{aligned} \quad (15)$$

Additionally, the effective resistance of the saturated porous medium at the REV scale can be calculated as

$$R_o = \frac{L_o}{\sigma A_{REV}} \quad (16)$$

where  $\sigma$  is the electrical conductivity of the water-saturated porous media.

The porosity of the REV is defined as the ratio of the total pore volume  $V_p$  and the total volume of the REV  $V_{REV}$  [e.g., Jackson, 2008, 2010]:

$$\phi = \frac{V_p}{V_{REV}} \quad (17)$$

Therefore, the porosity is calculated as

$$\begin{aligned} \phi &= \frac{\int_{r_{min}}^{r_{max}} \pi r^2 L_\tau(r) (-dN)}{A_{REV} L_o} = \frac{\int_{r_{min}}^{r_{max}} \pi r^2 r^{1-D_\tau} L_o^{D_\tau} D_f r_{max}^{D_f} r^{-D_f-1} dr}{A_{REV} L_o} \\ &= \frac{\pi L_o^{D_\tau-1} D_f r_{max}^{3-D_\tau}}{A_{REV} (3 - D_\tau - D_f)} (1 - \alpha^{3-D_\tau-D_f}) \end{aligned} \quad (18)$$

Consequently, the following is obtained

$$A_{REV} = \frac{\pi D_f L_o^{D_\tau-1} r_{max}^{3-D_\tau} (1 - \alpha^{3-D_\tau-D_f})}{\phi (3 - D_\tau - D_f)} \quad (19)$$

Combining Eq. (15), Eq. (16) and Eq. (19) yields

$$\begin{aligned} \sigma &= \frac{\phi r_{max}^{2D_\tau-2} (3 - D_\tau - D_f) \cdot (1 - \alpha^{D_\tau-D_f+1})}{L_o^{2D_\tau-2} \cdot (D_\tau - D_f + 1) \cdot (1 - \alpha^{3-D_\tau-D_f})} \cdot \sigma_w \\ &+ \frac{2\phi r_{max}^{2D_\tau-3} (3 - D_\tau - D_f) \cdot (1 - \alpha^{D_\tau-D_f})}{L_o^{2D_\tau-2} \cdot (D_\tau - D_f) \cdot (1 - \alpha^{3-D_\tau-D_f})} \cdot \Sigma_s \end{aligned} \quad (20)$$

This equation is the main contribution of this work. Eq. (20) indicates that the electrical conductivity of porous media under saturated conditions is explicitly related to the porosity, electrical conductivity of the pore liquid, and the microstructural parameters of a porous medium ( $D_f$ ,  $D_\tau$ ,  $\phi$ ,  $\alpha$ ,  $r_{max}$ ). Therefore, the model can reveal more mechanisms affecting the electrical conductivity of saturated porous media than other models available in literature. In particular, there is no empirical constant in Eq. (20) such as constants  $F$  or  $m$  in Archie model, for example. Eq. (20) can be rewritten as

$$\begin{aligned} \sigma &= \frac{\phi (3 - D_\tau - D_f) (1 - \alpha^{D_\tau-D_f+1})}{(\tau_g^{eff})^2 \cdot (D_\tau - D_f + 1) \cdot (1 - \alpha^{3-D_\tau-D_f})} \cdot \sigma_w \\ &+ \frac{2}{r_{max}} \frac{\phi (3 - D_\tau - D_f)}{(\tau_g^{eff})^2} \frac{(1 - \alpha^{D_\tau-D_f})}{(D_\tau - D_f) (1 - \alpha^{3-D_\tau-D_f})} \cdot \Sigma_s, \end{aligned} \quad (21)$$

where  $\tau_g^{eff}$  is the effective geometrical tortuosity of the medium resulting from the contributions of all the capillary tortuosities as presented above and is given by

$$\tau_g^{eff} = \left( \frac{L_o}{r_{max}} \right)^{D_\tau-1}. \quad (22)$$

Eq. (21) has the similar form to classical models reported by many authors [e.g., Waxman & Smits, 1968, Pride, 1994, Revil et al., 1998, Friedman, 2005, Linde et al., 2006, Glover, 2009, Brovelli & Cassiani, 2011] as following:

$$\sigma = g \cdot \sigma_w + h \cdot \sigma_s \quad (23)$$

where  $\sigma_s$  is the surface conductivity of porous media,  $g$  and  $h$  are two dimensionless geometrical factors, which depend on the texture of porous media.

The length of representative volume unit is related to the cross-section area of the REV by [Miao et al., 2016]

$$L_o^2 = A_{REV} \quad (24)$$

Note that  $L_o$  is not the length of sample but the side length of a representative unit as the REV is assumed to be a cube.

From Eq. (22) and Eq. (24), one has



$$\tau_g^{eff} = \left[ \frac{1 - \alpha^{3-D_\tau-D_f}}{\phi} \frac{\pi D_f}{3 - D_\tau - D_f} \right]^{\frac{D_\tau-1}{3-D_\tau}} \quad (25)$$

The fractal dimension for the tortuosity  $D_\tau$  can be approximately expressed as a function of properties of porous media as [Wei et al., 2015]

$$D_\tau = (3 - D_f) + (2 - D_f) \frac{\ln \frac{D_f}{D_f-1}}{\ln \phi} \quad (26)$$

When the surface conductivity is negligible, Eq. (21) becomes

$$\sigma = \frac{\phi(3 - D_\tau - D_f)(1 - \alpha^{D_\tau-D_f+1})}{(\tau_g^{eff})^2(D_\tau - D_f + 1)(1 - \alpha^{3-D_\tau-D_f})} \cdot \sigma_w \quad (27)$$

For a porous medium made up of straight parallel capillaries containing a fluid,  $D_\tau$  approaches 1. Therefore, the parameter  $\tau_g^{eff}$  is equal to 1 as indicated by Eq. (22) and Eq. (27) becomes  $\sigma = [\phi(2 - D_f)(1 - \alpha^{2-D_f})\sigma_w] / [(\tau_g^{eff})^2(2 - D_f)(1 - \alpha^{2-D_f})] = \phi\sigma_w / (\tau_g^{eff})^2 = \phi\sigma_w$ . This prediction is exactly what one would expect and is identical to the parallel model with one conducting phase and one insulating phase given by Gueguen & Palciauskas [1994]. Under that condition, Eq. (27) also corresponds to Archie's law by considering  $\phi = 1$ .

From Eq. (1) and Eq. (27), the formation factor is obtained as

$$F = \frac{(\tau_g^{eff})^2 (D_\tau - D_f + 1)(1 - \alpha^{3-D_\tau-D_f})}{\phi (3 - D_\tau - D_f)(1 - \alpha^{D_\tau-D_f+1})} \quad (28)$$

Similarly, Eq. (28) indicates that the formation factor is related to the porosity, and the microstructural parameters of a porous medium ( $D_f$ ,  $D_\tau$ ,  $\phi$ ,  $\alpha$ ). Additionally, Eq. (28) shows that the formation factor is inversely proportional to the porosity in the similar form as reported in Clennell [1997] (see his Eq. (17) and reference therein). It is seen from Eq. (28) that the formation factor can be considered independent of the grain size as indicated in the experimental results of Glover & Dery [2010], as long as the other geometrical parameters remain constant.

Even though the present model is based on the concept of capillary tubes, one can relate capillary radius to grain size. Indeed, in non consolidated granular materials, grain sizes and grain size distribution are much easier to obtain than pore sizes. Therefore, if a granular material is considered, Cai et al. [2012] proposed an expression to calculate maximum radius of the capillaries by combining the geometrical models of an equilateral-triangle and a square arrangement of spherical grains as

$$r_{max} = \frac{d}{8} \left[ \sqrt{\frac{2\phi}{1-\phi}} + \sqrt{\frac{\phi}{1-\phi}} + \sqrt{\frac{\pi}{4(1-\phi)}} - 1 \right], \quad (29)$$

where  $d$  is the mean grain diameter in porous media. Eq. (29) predicts that (1) when porosity approaches zero,  $r_{max}$  turns negative; (2) when porosity is approximately greater than 0.67,  $r_{max}$  becomes larger than mean grain radius. Those predictions are unrealistic. However, porosity of porous media is never zero and normally reported to be less than 0.45 [e.g., Waxman & Smits, 1968]. Therefore, the pore radius is typically less than grain radius as expected from the literature [e.g., Glover & Walker, 2009].

Table 1: Some of the models for the electrical conductivity of porous media used in this work for comparison. It should be noted that  $\sigma_m$  is the electrical conductivity of the solid matrix and taken as zero in this work.

Name	Equation	Reference
Archie model	$\sigma = \sigma_w \phi^m$	Archie [1942]
Parallel model	$\sigma = \phi \sigma_w + (1 - \phi) \sigma_m$	Gueguen & Palciauskas [1994]
Waff model	$\sigma = \frac{\sigma_w + (\sigma_m - \sigma_w)(1 - 2\phi/3)}{1 + \frac{\phi}{3}(\frac{\sigma_m}{\sigma_w} - 1)}$	Waff [1974]
Pride model	$\sigma = \frac{1}{F} [\sigma_w + (F - 1) \sigma_s]$	Pride [1994]
Revil model	$\sigma = \frac{\sigma_w}{F} [1 - t_{(+)}^f + F.Du + \frac{1}{2}(t_{(+)}^f - Du) \times (1 - \frac{Du}{t_{(+)}^f} + \sqrt{(1 - \frac{Du}{t_{(+)}^f})^2 + 4F \frac{Du}{t_{(+)}^f})]$	Revil et al. [1998]

## 4 Results and discussion

### 4.1 Sensitivity analysis of the new model

For modeling the electrical conductivity of saturated porous rocks as a function of the pore fluid electrical conductivity based on Eq. (21), one needs to know the fractal parameters  $\alpha$ ,  $D_f$ ,  $r_{max}$ ,  $\tau_{min}$  and  $D_\tau$ . It was generally recognized that the minimum pore radius is approximately two orders of magnitude smaller than the maximum pore radius in porous media. The value of  $\alpha = 0.01$  has been used in published articles [e.g., Cai et al., 2012, Liang et al., 2014, 2015]. Therefore, the value  $\alpha = 0.01$  is also used in this work for modeling. The fractal dimension  $D_f$  is determined via Eq. (9). If the pore size distribution of porous media is not known, the maximum radius  $r_{max}$  can be estimated via Eq. (29).  $D_\tau$  is obtained from Eq. (26) with the knowledge of  $D_f$  and  $\phi$ . From Eq. (25),  $\tau_g^{eff}$  is then determined. Substituting  $r_{max}$ ,  $D_f$ ,  $D_\tau$  and  $\tau_g^{eff}$  into Eq. (21), the electrical conductivity of porous samples is then determined with known values of  $\sigma_w$  and  $\Sigma_s$ .

Fig. 2 shows the variation of the electrical conductivity of porous media with the maximum pore radius predicted from the model presented by Eq. (21) for three different ratios of the minimum radius to the maximum radius of capillaries ( $\alpha = 0.01, 0.001$  and  $0.0001$ ) with  $\sigma_w = 3.0 \times 10^{-3}$  S/m,  $\Sigma_s = 0.5 \times 10^{-9}$  S and  $\phi = 0.4$ . It can be seen that when the ratio  $\alpha$  decreases, the electrical conductivity increases. This is attributed to the fact that the smaller ratio  $\alpha$  at given porosity causes the higher fractal dimension for pores as seen in Eq. (9). Additionally, the electrical conductivities of porous media for three different values of  $\alpha$  approach the constant and the same value at large grain diameters at which the surface electrical conductivity is negligible. This observation is in good agreement with what is predicted from Archie's law  $\sigma = \sigma_w \phi^m$  in which the electrical conductivity of porous media only depends on the porosity regardless of the grain size.

The proposed model indicated by Eq. (27) for the case of negligible surface conductivity is applied to predict the variation of the electrical conductivity of porous samples with porosity and compared with other models such as the Archie model [Archie, 1942],

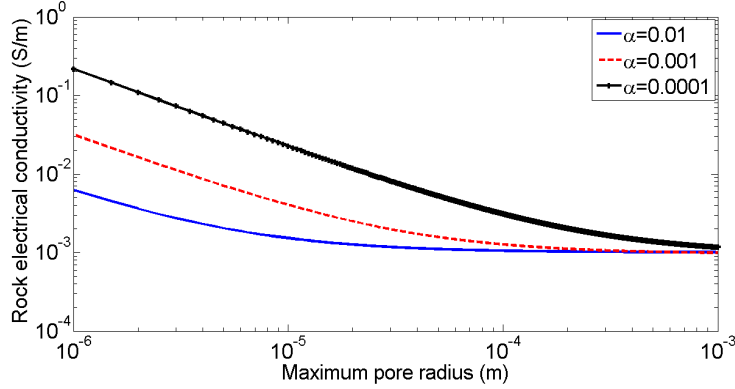


Figure 2: The variation of the electrical conductivity of porous samples with the maximum pore radius predicted from the model presented by Eq. (21) for three different values of  $\alpha$  (0.01, 0.001 and 0.0001) with  $\sigma_w = 3.0 \times 10^{-3}$  S/m,  $\Sigma_s = 0.5 \times 10^{-9}$  S and  $\phi = 0.4$ .

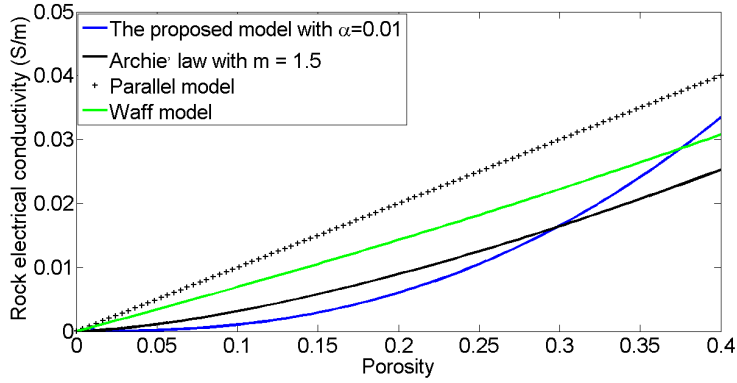


Figure 3: The variation of the electrical conductivity of porous samples with porosity predicted from different models with  $\sigma_w = 0.1$  S/m. For the proposed model shown by Eq. (27), the grain diameter is taken as  $50 \times 10^{-6}$  m and  $\alpha$  is taken as 0.01.

parallel model [Gueguen & Palciauskas, 1994], Waff model [Waff, 1974]. Table 1 lists some of the models for the electrical conductivity of porous media used in this work for comparison including the models given by Pride [1994], Revil et al. [1998]. The prediction from the models are performed with  $\sigma_w = 0.1$  S/m. The proposed model is applied with the grain diameter of  $50 \times 10^{-6}$  m and  $\alpha = 0.01$ . The comparison between those models is shown Fig. 3. It is seen that all the models have the similar behavior and indicate the increase of electrical conductivity of porous media with increasing porosity.

## 4.2 Effect of the pore water electrical conductivity

To compare the proposed model with experimental data available in literature, the input parameters corresponding to each sample are listed in Table 2

Fig. 4 shows the dependence of the electrical conductivity of saturated porous rocks as a function of the pore fluid electrical conductivity for six glass bead packs of different grain diameters experimentally obtained from Bolève et al. [2007] (see the symbols) and

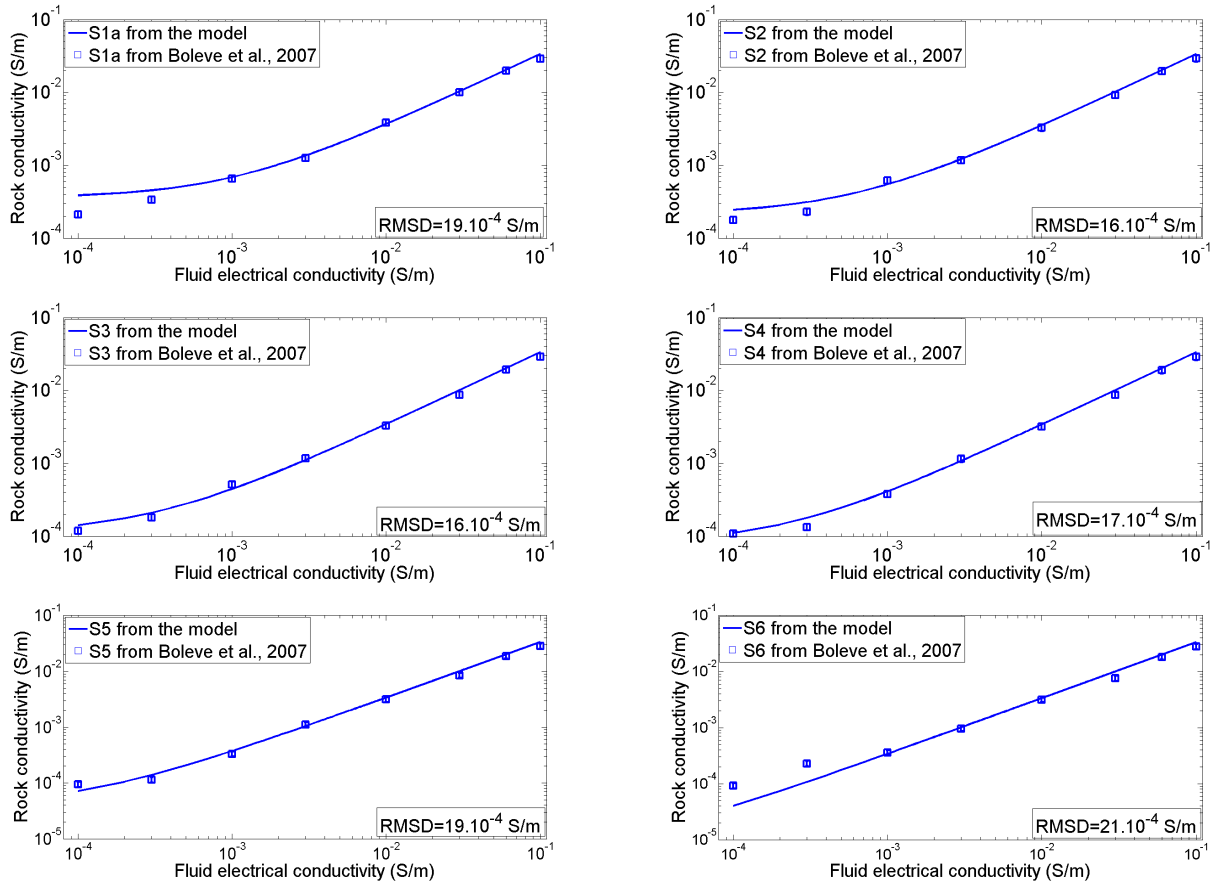


Figure 4: Electrical conductivity of different packs of glass bead versus the electrical conductivity of the fluid. The symbols are obtained from the work of Bolève et al. [2007]. The solid lines are from the proposed model presented by Eq. (21) with parameters given in Table 2.

Table 2: The parameters used in the proposed model to compare experimental data from different sources. Symbols of  $d$  ( $\mu\text{m}$ ),  $\phi$  (no units),  $\alpha$  (no units),  $\sigma_w$  (S/m) and  $\Sigma_s$  (S) stand for the grain diameter, porosity, ratio of minimum and maximum radius, fluid electrical conductivity and surface conductance of the fluid saturated porous samples, respectively

Sample	$d$ ( $\mu\text{m}$ )	$\phi$ (no units)	$\alpha$ (no units)	$\sigma_w$ (S/m)	$\Sigma_s$ (S)	source
S1a	56	0.4	0.01	$10^{-4}$ to 0.1	$0.5 \times 10^{-9}$	Bolève et al. [2007]
S2	93	0.4	0.01	$10^{-4}$ to 0.1	$0.5 \times 10^{-9}$	Bolève et al. [2007]
S3	181	0.4	0.01	$10^{-4}$ to 0.1	$0.5 \times 10^{-9}$	Bolève et al. [2007]
S4	256	0.4	0.01	$10^{-4}$ to 0.1	$0.5 \times 10^{-9}$	Bolève et al. [2007]
S5	512	0.4	0.01	$10^{-4}$ to 0.1	$0.5 \times 10^{-9}$	Bolève et al. [2007]
S6	3000	0.4	0.01	$10^{-4}$ to 0.1	$0.5 \times 10^{-9}$	Bolève et al. [2007]
SW	106	0.34	0.01	$10^{-5}$ to 1	$1.0 \times 10^{-9}$	Wildenschild et al. [2000]
FriedS	50, 100 200, 500	0.35-0.45	0.001	unused	0	Friedman & Robinson [2002]
ReS	250	0.04-0.23	0.0001	unused	unused	Revil et al. [2014]

the prediction from the model presented by Eq. (21) (the solid lines). Mean grain size of six glass bead packs denoted by S1a, S2, S3, S4, S5 and S6 are  $56 \mu\text{m}$ ,  $93 \mu\text{m}$ ,  $181 \mu\text{m}$ ,  $256 \mu\text{m}$ ,  $512 \mu\text{m}$  and  $3000 \mu\text{m}$ , respectively (see Table 2). The measured porosity of the packs was reported to be  $\phi = 0.40$  irrespective of the size of the glass beads [Bolève et al., 2007]. By fitting experimental data shown in Fig. 4, the surface conductance is found to be  $\Sigma_s = 0.5 \times 10^{-9}$  S for all samples. This value is of the same order of magnitude as that reported in literature for the silica surface in contact with the NaCl electrolyte (e.g.,  $\Sigma_s = 8.9 \times 10^{-9}$  S [Revil & Glover, 1998] or  $\Sigma_s = 4.0 \times 10^{-9}$  S [Glover & Dery, 2010] or  $\Sigma_s = 5.3 \times 10^{-9}$  S [Bull & Gortner, 1932] or  $\Sigma_s = 1.4 \times 10^{-9}$  S [Lorne et al., 1999]). The root-mean-square deviation (RMSD) calculated for all samples S1a, S2, S3, S4, S5 and S6 are  $19 \times 10^{-4}$  S/m,  $16 \times 10^{-4}$  S/m,  $16 \times 10^{-4}$  S/m,  $17 \times 10^{-4}$  S/m,  $19 \times 10^{-4}$  S/m and  $21 \times 10^{-4}$  S/m, respectively. The results show that the predictions from the model are in very good agreement with the experimental data. The model is able to reproduce the main trend of experimental data and especially at high fluid electrolyte concentration and large grain size. The misfit of the model with experimental data at low electrolyte concentration can be explained by the possible exchange of the electrical current between the electrical double layer and bulk fluid [Daigle et al., 2015]. As seen in Fig. 4, at high fluid electrical conductivity there is a linear dependence. The reason is that at high fluid electrical conductivity or large grain size, the electrical conductivity of saturated porous samples  $\sigma$  is linearly related to the fluid electrical conductivity  $\sigma_w$  as presented in Eq. (1) or Eq. (27), that is  $Du \ll 1$ .

The dependence of the electrical conductivity of another saturated sand pack (denoted by SW) as a function of the pore fluid electrical conductivity from a different source [Wildenschild et al., 2000] is also shown in Fig. 5. The symbols are from the reported data and the solid line is predicted from the model with the parameters given in Table 2 in which the mean diameter of grains of a sand pack is deduced from Glover & Walker

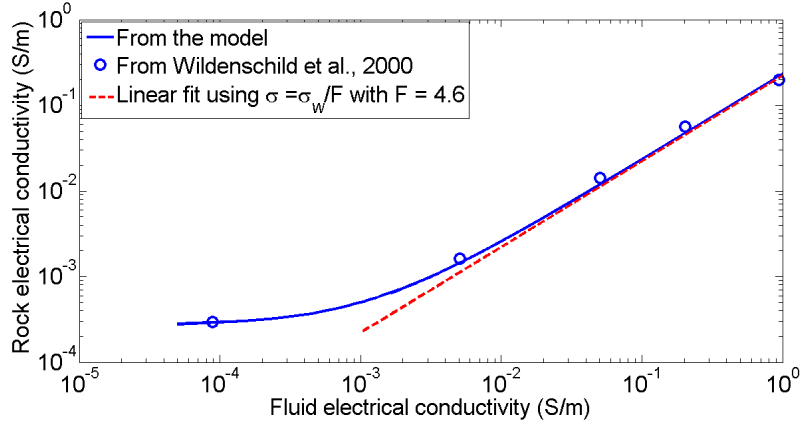


Figure 5: Electrical conductivity of a porous sample versus the electrical conductivity of the fluid. The symbols are obtained from Wildenschild et al. [2000]. The solid line is predicted from the model indicated by Eq. (21) with parameters given in Table 2. The RMSD is  $90 \times 10^{-4}$  S/m. The dashed line is linear fitting using the relation  $\sigma = \sigma_w / F$  with  $F = 4.6$ .

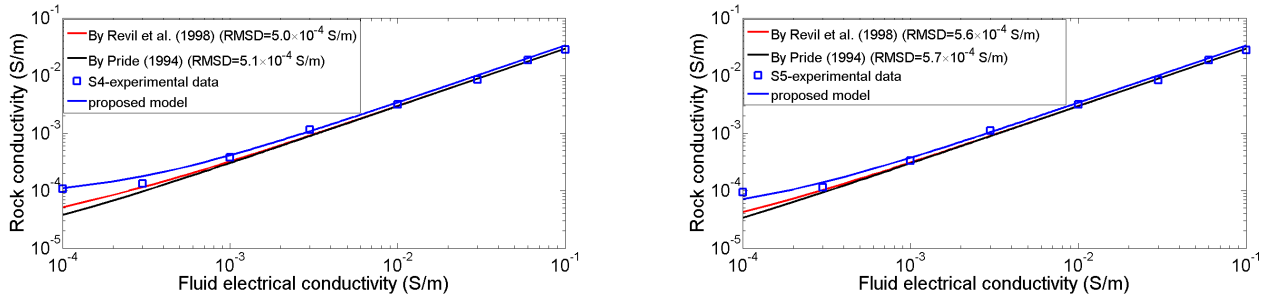


Figure 6: The variation of electrical conductivity of saturated porous media with the electrical conductivity of the fluid predicted from the proposed model indicated by Eq. (21) and other models given by Pride [1994], Revil et al. [1998].

[2009]

$$d = 2\theta\sqrt{8kF} \quad (30)$$

where  $\theta$  is the theta transform (unitless) and equal to 3.436 for spherical grain samples,  $k$  and  $F$  are the permeability and formation factor of porous samples, respectively ( $k = 6.16 \times 10^{-12}$  m<sup>2</sup> and  $F = 4.9$  for the sample SW as reported in Wildenschild et al. [2000]). Consequently,  $d$  is calculated to be 106  $\mu$ m. The linear trend of the curve (the dashed line) can be used to determine the formation factor. One can obtain  $\sigma = \sigma_w / 4.6$  for the dashed line in Fig. 5. Consequently, the formation factor is 4.6. This theoretically predicted value is in good agreement with the measured value of 4.9 from Wildenschild et al. [2000]. The RMSD in this case is  $90 \times 10^{-4}$  S/m that is larger than those of consolidated samples as reported above.

The variation of electrical conductivity of saturated porous media with the electrical conductivity of the fluid predicted from the model is also compared with other models

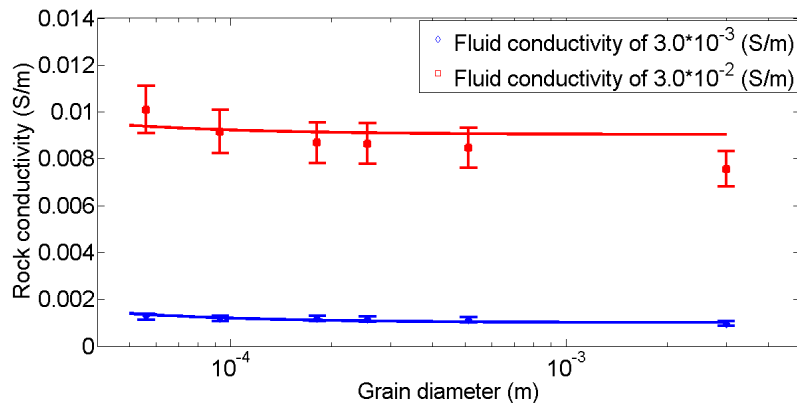


Figure 7: Electrical conductivity of porous samples versus the grain diameter of the samples at two different electrical conductivity of the fluid ( $3.0 \times 10^{-3}$  and  $3.0 \times 10^{-2}$  S/m). Mean grain size of six glass bead packs are 56, 93, 181, 256, 512, and 3000  $\mu\text{m}$ , respectively. The porosity of all of the packs is 0.4. The symbols are obtained from Bolève et al. [2007]. The solid lines are predicted from the model indicated by Eq. (21) with parameters given in Table 2.

available in literature [e.g., Pride, 1994, Revil et al., 1998] (see Table 1) as shown in Fig. 6. Input parameters for modeling are the same as those used in Fig. 4 for the representative samples S4 and S5 whose data are also shown in Fig. 6. Additionally,  $t_{(+)}^f$  is taken as 0.38 corresponding to NaCl solution [Revil et al., 1998],  $\sigma_s$  is calculated by  $6\Sigma_s/d$  ( $d$  is grain diameter) [Linde et al., 2006, Bolève et al., 2007] and  $F$  is taken as 3.4 for both samples S4 and S5 [Bolève et al., 2007]. The RMSD of the fits from Revil et al. [1998] and Pride [1994] for samples S4 and S5 are  $5.0 \times 10^{-4}$  S/m and  $5.1 \times 10^{-4}$  S/m;  $5.6 \times 10^{-4}$  S/m and  $5.7 \times 10^{-4}$  S/m, respectively. It is shown that the proposed model is in good agreement with those given by Pride [1994] and Revil et al. [1998], especially at high fluid electrical conductivity (Dukhin number  $Du \leq 0.004$ ).

### 4.3 Effect of the textural parameters of the porous medium

The dependence of the electrical conductivity of saturated porous media on the grain diameter is also predicted using the procedure mentioned in section 4.2. The prediction is shown by the solid lines in Fig. 7 for two different fluid conductivities ( $3.0 \times 10^{-3}$  S/m and  $3.0 \times 10^{-2}$  S/m). The theoretical results are then compared with the measured values obtained from Bolève et al. [2007] (see symbols). It should be noted that the input parameters for modeling are reported in Table 2 for Bolève et al. [2007]. The uncertainties of the measured electrical conductivities of porous samples and grain diameter are reported to be roughly 10 % by Bolève et al. [2007]. Therefore, a  $\pm 10$  % error is used for the experimental data shown in Fig. 7. The comparison shows that the model is able to reproduce the main trend of the experimental data. However, it is seen that the fit at lower fluid conductivity is not as good as at higher one. The reason is that the assumption of the conduction current path in parallel may be not truly valid at low electrolyte concentration [Daigle et al., 2015].

Figure 8 shows the ratio of the electrical conductivity of the glass bead samples to that

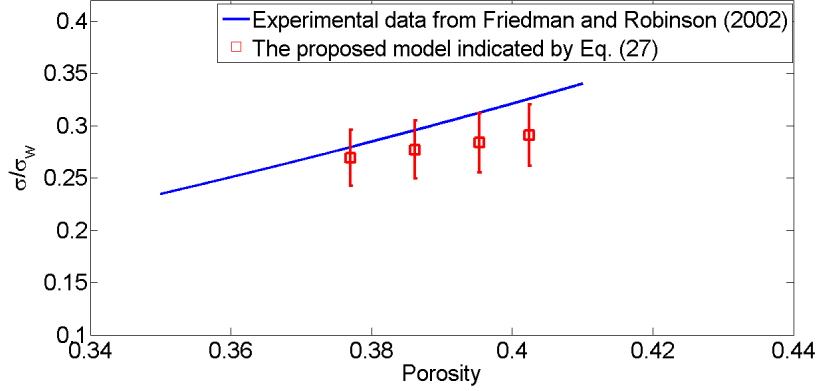


Figure 8: Ratio of the electrical conductivity of the glass bead sample to that of the electrolyte as a function of the porosity. Mean grain size of four samples are 50, 100, 200, and 500  $\mu\text{m}$ , respectively. The symbols are obtained from Friedman & Robinson [2002] with  $\pm 10\%$  uncertainty. The solid line is from the proposed model given by Eq. (27) with parameters given in Table 2.

of the electrolyte as a function of the porosity experimentally obtained from Friedman & Robinson [2002] (see symbols) for four samples of spherical glass beads with diameters of 50, 100, 200 and 500  $\mu\text{m}$  denoted by FriedS in Table 2. This measured result can be explained by the model (Eq. (27)) with input parameters given in Table 2. The surface conductivity is negligible as stated in Friedman & Robinson [2002]. A  $\pm 10\%$  error is used for the experimental data shown in Figure 8. The result shows that the prediction of the model is close to the experimental data.

#### 4.4 Formation factor and hydraulic tortuosity

The variation of the formation factor of the porous media with the grain diameter can be predicted from Eq. (28) as shown in Fig. 9 (the solid line). The parameters for modeling are  $\alpha = 0.01$  and  $\phi = 0.40$  that are compatible with glass bead packs reported in Bolève et al. [2007] (see Table 2). The formation factor measured by Bolève et al. [2007] for different grain diameters is also shown by the symbols in Fig. 9. It is seen that the model is in good agreement with experimental data. According to Archie model [Archie, 1942], the formation factor  $F$  is linked to the porosity  $\phi$  ( $\phi = 0.40$  irrespective of the size of the glass beads as stated in Bolève et al. [2007]) by  $F = \phi^{-m}$ . For unconsolidated samples made of perfect spheres, the exponent should be constant (1.5) [Sen et al., 1981a]. Consequently,  $F$  is predicted to be independent of the grain size. This constant value of formation factor predicted by the model in Eq. (28) ( $F = 3.21$ ) is in very good agreement with the value measured by Bolève et al. [2007] ( $3.4 \pm 0.2$ ) for glass beads.

The variation of the formation factor of the porous media with porosity experimentally obtained for a set of core samples of the Fontainebleau sandstone [Revil et al., 2014] is shown in Fig. 10 (see the symbols). The main experimental trend can be explained by the model indicated by Eq. (28) (the solid line). The value of  $\alpha = 0.0001$  is used for modeling because of the best fit and that value is also used to fit experimental data for Fontainebleau sandstone [e.g., Liang et al., 2014]. The mean grain diameter is  $d = 250 \mu\text{m}$



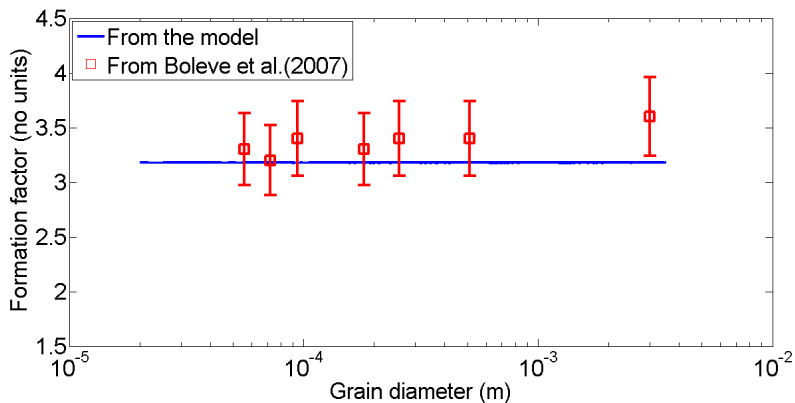


Figure 9: The variation of the formation factor with the grain diameter. The symbols are obtained from Bolève et al. [2007]. The solid line is predicted from the model indicated by Eq. (28) with parameters given in Table 2 for the source of Bolève et al. [2007] with  $\pm 10\%$  uncertainty on the experimental data.

obtained from CT scans in Revil et al. [2014] (see sample ReS in Table 2). It is indicated that the model can produce the main behavior of the experimental data given by Revil et al. [2014]. However, a deviation is observed at very low porosity (less than 15%). The reason may be that the model is developed based on porous media made up of mono-sized spherical grains [Liang et al., 2015]. However, for the consolidated samples of the Fontainebleau sandstone, the rock texture consists of mineral grains of various shapes and sizes and its pore structure is extremely complex. The formula for the fractal dimension  $D_f$ , the maximum radius  $r_{max}$  determined from the grain diameter, porosity may not be suitable. Additionally, another reason for a deviation is the variation of  $\alpha$  from sample to sample (for modeling,  $\alpha = 0.0001$  is applied for all samples).

Based on Eq. (28), the effective electrical tortuosity is defined as [e.g., Clennell, 1997]

$$(\tau_e^{eff})^2 = F\phi = (\tau_g^{eff})^2 \frac{(D_\tau - D_f + 1)(1 - \alpha^{3-D_\tau-D_f})}{(3 - D_\tau - D_f)(1 - \alpha^{D_\tau-D_f+1})} \quad (31)$$

Eq. (31) is used to predict the effective electrical tortuosity of 12 samples of glass beads with different diameters reported in Glover & Dery [2010]. The input parameters for modeling and predicted values for all samples are listed in Table 3. It is seen that the mean value over 12 samples is around 1.11 and that is smaller than the hydraulic tortuosity of those samples predicted by Guarracino & Jougnot [2018] using different approaches ( $\tau_h^{av} = (1.2+1.4)/2 = 1.3$ ). The result is in good agreement with [Ghanbarian et al., 2013]. This work provides a possible link between different properties. For example, the hydraulic conductivities of porous media can be deduced from electrical conductivities [e.g., Doussan & Ruy, 2009, Jougnot et al., 2010, Niu et al., 2015].

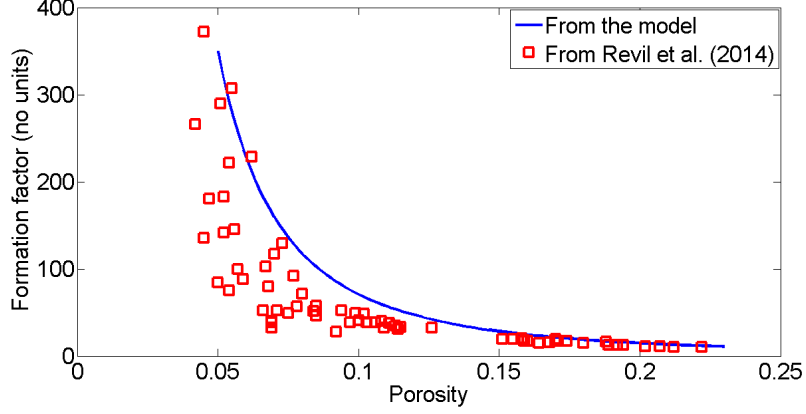


Figure 10: The variation of the formation factor with with porosity. The symbols are obtained from Revil et al. [2014]. The solid line is predicted from the model indicated by Eq. (28) with input parameters given in Table 2.

Table 3: Input parameters for modeling and predicted hydraulic tortuosities. Grain diameter ( $d$  in  $\mu\text{m}$ ) and porosity ( $\phi$ ) are taken from Glover & Dery [2010]

Sample number	$d$	$\phi$	$\alpha$	$\tau_e^{eff}$
1	1.05	0.411	0.01	1.072
2	2.11	0.398	0.01	1.098
3	5.01	0.385	0.01	1.125
4	11.2	0.401	0.01	1.092
5	21.5	0.383	0.01	1.128
6	31.0	0.392	0.01	1.110
7	47.5	0.403	0.01	1.088
8	104	0.394	0.01	1.106
9	181	0.396	0.01	1.102
10	252	0.414	0.01	1.067
11	494	0.379	0.01	1.137
12	990	0.391	0.01	1.111
mean				1.110

## 5 Conclusions

A physically based model for estimating electrical conductivity of saturated porous media has been developed in this work. The model is derived assuming that the porous media can be represented by a bundle of tortuous capillary tubes with a fractal pore-size distribution. The proposed model is explicitly related to electrical conductivity of the pore liquid and the microstructural parameters of a porous medium ( $D_f$ ,  $D_\tau$ ,  $\phi$ ,  $\alpha$ ,  $r_{max}$ ). Therefore, the model can reveal more mechanisms affecting the electrical conductivity of porous media than other models available in literature. From the model, the expressions for the formation factor and hydraulic tortuosity are also obtained.

The model's sensitivity to its parameter is first tested. Then, it is compared with previously published models and experimental data. The proposed model is consistent with previous ones from the literature. The results predicted by the model are in very good agreement with experimental data, especially for unconsolidated samples. The proposed model is the first fractal theory based one to take the surface conductivity into account. This simple analytical model opens-up new possibilities for predicting the electrical conductivity of porous media and link it with hydraulic conductivity. The analytical development of a model for partially saturated porous media using the presented approach will be carried out in the near future.

## References

- Archie, G. E., 1942. The electrical resistivity log as an aid in determining some reservoir characteristics, *Petroleum Transactions of AIME*, **146**, 54–62.
- Binley, A. & Kemna, A., 2005. *DC Resistivity and Induced Polarization Methods*. In: Rubin Y., Hubbard S.S. (eds) *Hydrogeophysics*, Springer.
- Binley, A., Hubbard, S. S., Huisman, J. A., Revil, A., Robinson, D. A., Singha, K., & Slater, L. D., 2015. The emergence of hydrogeophysics for improved understanding of subsurface processes over multiple scales, *Water Resources Research*, **51**(6), 3837–3866.
- Bo-Ming, Y., 2005. Fractal character for tortuous streamtubes in porous media, *Chinese Physics Letters*, **22**(1), 158–160.
- Bolève, A., Crespy, A., Revil, A., Janod, F., & Mattiuzzo, J. L., 2007. Streaming potentials of granular media: Influence of the dukhin and reynolds numbers, *Journal of Geophysical Research*, **B08204**(112).
- Brovelli, A. & Cassiani, G., 2011. Combined estimation of effective electrical conductivity and permittivity for soil monitoring, *Water Resources Research*, **47**(8).
- Brovelli, A., Cassiani, G., Dalla, E., Bergamini, F., Pitea, D., & Binley, A. M., 2005. Electrical properties of partially saturated sandstones: Novel computational approach with hydrogeophysical applications, *Water Resources Research*, **41**(8).
- Bull, H. B. & Gortner, R. A., 1932. Electrokinetic potentials. X. The effect of particle size on the potential, *Journal of Physical Chemistry*, **36**(1), 111–119.

- Bussian, A. E., 1983. Electrical conductance in a porous medium, *Geophysics*, **48**(9), 1258–1268.
- Cai, J., Wei, W., Hu, X., & Wood, D. A., 2017. Electrical conductivity models in saturated porous media: A review, *Earth Science Reviews*, **171**, 419–433.
- Cai, J. C., Hu, X. Y., Standnes, D. C., & You, L. J., 2012. An analytical model for spontaneous imbibition in fractal porous media including gravity, *Colloids and Surfaces, A: Physicochemical and Engineering Aspects*, **414**, 228–233.
- Carpenter, P. J., Ding, A., Cheng, L., Liu, P., & Chur, F., 2009. Apparent formation factor for leachate-saturated waste and sediments: Examples from the usa and china, *Journal of Earth Science*, **20**(3), 606.
- Clennell, M. B., 1997. Tortuosity: a guide through the maze, *Geological Society, London, Special Publications*, **122**(1), 299–344.
- Coleman, S. W. & Vassilicos, J. C., 2008a. Tortuosity of unsaturated porous fractal materials, *Phys. Rev. E*, **78**, 016308.
- Coleman, S. W. & Vassilicos, J. C., 2008b. Transport properties of saturated and unsaturated porous fractal materials, *Phys. Rev. Lett.*, **100**, 035504.
- Daigle, H., Ghanbarian, B., Henry, P., & Conin, M., 2015. Universal scaling of the formation factor in clays: Example from the nankai trough, *Journal of Geophysical Research: Solid Earth*, **120**(11), 7361–7375.
- Doussan, C. & Ruy, S., 2009. Prediction of unsaturated soil hydraulic conductivity with electrical conductivity, *Water Resources Research*, **45**(10).
- Doyen, P. M., 1988. Permeability, conductivity, and pore geometry of sandstone, *Journal of Geophysical Research: Solid Earth*, **93**(B7), 7729–7740.
- Dukhin, S. & Shilov, V., 1974. *Dielectric Phenomena and the Double Layer in Disperse Systems and Polyelectrolytes*, John Wiley and Sons, New York.
- Ellis, M. H., Sinha, M. C., Minshull, T. A., Sothcott, J., & Best, A. I., 2010. An anisotropic model for the electrical resistivity of two-phase geologic materials, *Geophysics*, **75**(6), E161–E170.
- Feder, J. & Aharony, A., 1989. *Fractals in Physics*, North Holland, Amsterdam.
- Friedman, S. P., 2005. Soil properties influencing apparent electrical conductivity: a review, *Computers and Electronics in Agriculture*, **46**(1), 45 – 70.
- Friedman, S. P. & Robinson, D. A., 2002. Particle shape characterization using angle of repose measurements for predicting the effective permittivity and electrical conductivity of saturated granular media, *Water Resources Research*, **38**(11), 1–11.
- Ghanbarian, B., Hunt, A., P. Ewing, R., & Sahimi, M., 2013. Tortuosity in porous media: A critical review, *Soil Science Society of America Journal*, **77**(5), 1461–1477.

- Ghanbarian, B., Hunt, A. G., Ewing, R. P., & Skinner, T. E., 2014. Universal scaling of the formation factor in porous media derived by combining percolation and effective medium theories, *Geophysical Research Letters*, **41**(11), 38843890.
- Ghanbarian-Alavijeh, B., Millan, H., & Huang, G., 2011. A review of fractal, prefractal and pore-solid-fractal models for parameterizing the soil water retention curve, *Canadian Journal of Soil Science*, **91**(1), 1–14.
- Glover, P., 2009. What is the cementation exponent? a new interpretation, *The Leading Edge*, **28**(1), 82–85.
- Glover, P., 2015. Geophysical properties of the near surface earth: Electrical properties, *Treatise on Geophysics*, **11**, 89–137.
- Glover, P., Gomez, J., Meredith, P., Hayashi, K., Sammonds, P., & Murrell, S., 1997. Damage of saturated rocks undergoing triaxial deformation using complex electrical conductivity measurements: Experimental results, *Physics and Chemistry of the Earth*, **22**(1), 57 – 61.
- Glover, P. W. J. & Dery, N., 2010. Streaming potential coupling coefficient of quartz glass bead packs: Dependence on grain diameter, pore size, and pore throat radius, *Geophysics*, **75**(6), F225–F241.
- Glover, P. W. J. & Walker, E., 2009. Grain-size to effective pore-size transformation derived from electrokinetic theory, *Geophysics*, **74**(1), E17–E29.
- Guarracino, L. & Jougnot, D., 2018. A physically based analytical model to describe effective excess charge for streaming potential generation in water saturated porous media, *Journal of Geophysical Research: Solid Earth*, **123**(1), 52–65.
- Gueguen, Y. & Palciauskas, V., 1994. *Introduction to the Physics of Rocks*, Princeton University Press.
- Hanai, T., 1961. Theory of the dielectric dispersion due to the interfacial polarization and its application to emulsions, *Colloid and Polymer Science*, **171**(1), 23.
- Herrick, D. C. & Kennedy, W. D., 1994. Electrical efficiency a pore geometric theory for interpreting the electrical properties of reservoir rocks, *Geophysics*, **59**(6), 918–927.
- Hubbard, S. & Rubin, Y., 2005. *Introduction to Hydrogeophysics*. In: Rubin Y., Hubbard S.S. (eds) *Hydrogeophysics*. Water Science and Technology Library, Springer.
- Hunt, A. G., 2004. Continuum percolation theory and archie’s law, *Geophysical Research Letters*, **31**(19), L19503 1–4.
- Jackson, M. D., 2008. Characterization of multiphase electrokinetic coupling using a bundle of capillary tubes model, *Journal of Geophysical Research: Solid Earth*, **113**(B4).
- Jackson, M. D., 2010. Multiphase electrokinetic coupling: Insights into the impact of fluid and charge distribution at the pore scale from a bundle of capillary tubes model, *Journal of Geophysical Research: Solid Earth*, **115**(B7).

- Jougnot, D., Revil, A., Lu, N., & Wayllace, A., 2010. Transport properties of the callovo-oxfordian clay rock under partially saturated conditions, *Water Resources Research*, **46**(8).
- Katz, A. J. & Thompson, A. H., 1985. Fractal sandstone pores: Implications for conductivity and pore formation, *Phys. Rev. Lett.*, **54**, 1325–1328.
- Laloy, E., Javaux, M., Vanclooster, M., Roisin, C., & Bielders., C. L., 2011. Electrical resistivity in a loamy soil: Identification of the appropriate pedo-electrical model, *Vadose Zone Journal*, **10**, 1023–1033.
- Liang, M., Yang, S., & Yu, B., 2014. A fractal streaming current model for charged microscale porous media, *Journal of Electrostatics*, **72**.
- Liang, M., Yang, S., Miao, T., & Yu, B., 2015. Analysis of electroosmotic characters in fractal porous media, *Chemical Engineering Science*, **127**.
- Linde, N., Binley, A., Tryggvason, A., Pedersen, L. B., & Revil, A., 2006. Improved hydrogeophysical characterization using joint inversion of cross-hole electrical resistance and ground-penetrating radar traveltime data, *Water Resources Research*, **42**(12).
- Lorne, B., Perrier, F., & Avouac, J. P., 1999. Streaming potential measurements: 1. properties of the electrical double layer from crushed rock samples, *Journal of Geophysical Research*, **104**(B8), 17.857–17.877.
- Mandelbrot, B. B., 1982. *The Fractal Geometry of Nature*, W.H. Freeman, New York.
- McLachlan, D. S., Button, M. B., Adams, S. R., Gorringer, V. M., Kneen, J. D., Muoe, J., & Wedepohl, E., 1987. Formation resistivity factors for a compressible solidbrine mixture, *Geophysics*, **52**(2), 194–203.
- Miao, T., Cheng, S., Chen, A., & Yu, B., 2016. Analysis of axial thermal conductivity of dual-porosity fractal porous media with random fractures, *International Journal of Heat and Mass Transfer*, **102**, 884 – 890.
- Niu, Q., Fratta, D., & Wang, Y.-H., 2015. The use of electrical conductivity measurements in the prediction of hydraulic conductivity of unsaturated soils, *Journal of Hydrology*, **522**, 475 – 487.
- Pape, H., Riepe, L., & Schopper, J. R., 1987. Theory of self-similar network structures in sedimentary and igneous rocks and their investigation with microscopical and physical methods, *Colloid and Polymer Sciencel*, **148**(2), 121–147.
- Pfannkuch, H. O., 1972. On the correlation of electrical conductivity properties of porous systems with viscous flow transport coefficients, *Developments in Soil Science*, **2**, 42 – 54.
- Pride, S., 1994. Governing equations for the coupled electromagnetics and acoustics of porous media, *Physical Review B*, **50**(21), 15678–15696.

- Revil, A. & Glover, P. W. J., 1997. Theory of ionic-surface electrical conduction in porous media, *Physical Review B*, **55**(3), 1757–1773.
- Revil, A. & Glover, P. W. J., 1998. Nature of surface electrical conductivity in natural sands, sandstones, and clays, *Geophysical Research Letters*, **25**(5), 691–694.
- Revil, A., Cathles III, L. M., Losh, S., & Nunn, J. A., 1998. Electrical conductivity in shaly sands with geophysical applications, *Journal of Geophysical Research: Solid Earth*, **103**(B10), 23925–23936.
- Revil, A., Pezard, P. A., & Glover, P. W. J., 1999. Streaming potential in porous media 1. theory of the zeta potential, *Journal of Geophysical Research*, **104**(B9), 20021–20031.
- Revil, A., Karaoulis, M., Johnson, T., & Kemna, A., 2012. Review: Some low-frequency electrical methods for subsurface characterization and monitoring in hydrogeology, *Hydrogeology Journal*, **20**(4), 617–658.
- Revil, A., Kessouri, P., & Torres-Verdin, C., 2014. Electrical conductivity, induced polarization, and permeability of the fontainebleau sandstone, *Geophysics*, **79**(5), D301–D318.
- Roy, S. & Tarafdar, S., 1997. Archie’s law from a fractal model for porous rocks, *Phys. Rev. B*, **55**, 8038–8041.
- Sahimi, M., 1993. Flow phenomena in rocks: from continuum models to fractals, percolation, cellular automata, and simulated annealing, *Rev. Mod. Phys.*, **65**, 1393–1534.
- Sen, P., Scala, C., & Cohen, M. H., 1981a. A self-similar model for sedimentary rocks with application to the dielectric constant of fused glass beads, *Journal of the Soil Mechanics and foundations Division*, **46**(5), 781–795.
- Sen, P. N., Scala, C., & Cohen, M. H., 1981b. A selfsimilar model for sedimentary rocks with application to the dielectric constant of fused glass beads, *Geophysics*, **46**(5), 781–795.
- Speight, J. G., 2011. *An Introduction to Petroleum Technology, Economics, and Politics*, John Wiley and Sons.
- Street, N., 1961. *Electrokinetics III: surface conductance and the conductive solids effect*, Urbana: Illinois State Geological Survey.
- Thanh, L. D., Van Do, P., Van Nghia, N., & Ca, N. X., 2018. A fractal model for streaming potential coefficient in porous media, *Geophysical Prospecting*, **66**(4), 753–766.
- Thompson, A., Katz, A., & Krohn, C., 1987. The microgeometry and transport properties of sedimentary rock, *Advances in Physics*, **36**(5), 625–694.
- Thompson, A. H., 1991. Fractals in rock physics, *Annual Review of Earth and Planetary Sciences*, **19**(1), 237–262.

- Waff, H. S., 1974. Theoretical considerations of electrical conductivity in a partially molten mantle and implications for geothermometry, *Journal of Geophysical Research*, **79**(26), 4003–4010.
- Wang, L., Mao, Z., Shi, Y., Tao, Q., Cheng, Y., & Song, Y., 2014. A novel model of predicting archie’s cementation factor from nuclear magnetic resonance (nmr) logs in low permeability reservoirs, *Journal of Earth Science*, **25**(1), 183–188.
- Waxman, M. H. & Smits, L. J. M., 1968. Electrical conductivities in oil bearing shaly sands, *Society of Petroleum Engineers Journal*, **8**, 107–122.
- Wei, W., Cai, J., Hu, X., & Han, Q., 2015. An electrical conductivity model for fractal porous media, *Geophysical Research Letters*, **42**(12), 4833–4840.
- Wildenschild, D., Roberts, J. J., & Carlberg, E. D., 2000. On the relationship between microstructure and electrical and hydraulic properties of sand-clay mixtures, *Geophysical Research Letters*, **27**(19), 3085–3088.
- Woodruff, W. F. & Revil, A., 2011. Ccc-normalized clay-water sorption isotherm, *Water Resources Research*, **47**(11).
- Wu, J. & Yu, B., 2007. A fractal resistance model for flow through porous media, *International Journal of Heat and Mass Transfer*, **50**(19), 3925 – 3932.
- Xu, P., 2015. A discussion on fractal models for transport physics of porous media, *Fractals*, **23**(3), 15300011–153000111.
- Yu, B. & Cheng, P., 2002a. A fractal permeability model for bi-dispersed porous media, *International Journal of Heat and Mass Transfer*, **45**(14), 2983–2993.
- Yu, B. & Cheng, P., 2002b. A fractal permeability model for bi-dispersed porous media, *International Journal of Heat and Mass Transfer*, **45**(14), 2983 – 2993.
- Yu, B., Lee, L. J., & Cao, H., 2001. Fractal characters of pore microstructures of textile fabrics, *Fractals*, **09**(02), 155–163.